COMPUTATIONAL FLUID DYNAMICS ANALYSIS OF NO_x AND OTHER POLLUTANTS IN THE MAN B&W 7S50MC MARINE ENGINE AND EFFECT OF EGR AND WATER ADDITION

M I Lamas; C G Rodríguez and **H P Aas.** Universidade da Coruña, Spain

SUMMARY

Marine engines represent a significant contribution to global emissions. In order to overcome this problem, a great attention was given to reduce their exhaust emissions in the last years, and marine engines have to adapt to regional, national and international restrictions. In this regard, the purpose of this paper is to develop a numerical model to study NO_x (oxides of nitrogen) and other pollutants in engines. EGR and water addition were studied too as measures to reduce NO_x. The main advantage of this study is that it provides a cheap and fast method to analyze emissions, contrary to experimental setups which are too expensive and laborious. Particularly, a commercial marine engine was analyzed and validated with experimental data. Results showed that increasing EGR and water addition leads to reduce NO_x, but increase carbon monoxide and unburnt hydrocarbons due to an incomplete combustion.

NOMENCLATURE

b	Cylinder bore (m)
f	Mixture fraction (-)
f_{NO}	Mass fraction of NO (-)
h	Heat transfer coefficient (W m^{-2} K^{-1})
H	Enthalpy (J/kg)
k	Thermal conductivity (W m^{-1} K^{-1})
k_i	Rate constant (m^3 gmol^{-1} s^{-1})
p	Pressure (Pa)
t	Time (s)
T	Temperature (K)
u	Velocity (m s^{-1})

Greek symbols

μ	Dynamic viscosity (Pa s)
μ_t	Turbulent viscosity (Pa s)
ν	Kinematic viscosity (m^2 s^{-1})
ρ	Density (kg m^{-3})
σ	Prandtl number (-)
σ_h	Turbulent Prandtl number (-)
σ_ζ	Turbulent Schmidt number (-)
τ_{ij}	Stress tensor (Pa)

1. INTRODUCTION

Nowadays, environmental pollution is increasing at an alarming rate. Transportation represents one of the main sources of emissions in the world, especially regarding carbon dioxide (CO_2), carbon monoxide (CO), nitrogen oxides (NO_x), sulfur oxides (SO_x), hydrocarbons (HC) and particulates. Particularly, marine diesel engines emit significant levels of CO_2, SO_x and NO_x. Studies show that emissions of CO_2, SO_x and NO_x from ships correspond to about 2, 4, and 11% of the global anthropogenic emissions, respectively, Skjølsvik *et al.* [1].

Although nowadays there is a wide range of sophisticated experimental techniques to analyze emissions from engines, computational fluid dynamics (CFD) offers a cheaper and faster alternative to study the combustion process and composition of the exhaust gases. CFD is a branch of fluid mechanics based on the subdivision of the computational domain into small elements overlaying the whole domain. For each subdivision, the governing equations are solved using numerical methods. Concerning combustion, CFD can provide detailed information that can not be determined by experimental techniques. Regarding to this, several works about simulation of small two and four-stroke engines can be found in the literature. Some of them are validations of numerical models, comparing the results of CFD with experimental measurements of the exhaust gases composition [2-6]. Other works are applications of CFD to reduce emissions. In this regard, a pollutant reduction measurement which has extensively studied by CFD was split injection [7-10]. Other pollutant reduction measurements analyzed numerically were the modification of the combustion chamber geometry [11-12] and number of injectors [13].

These models about small engines can be applied to medium and large marine engines. Nevertheless, the simulation of the combustion process of large and medium marine engines is more complicated. The main difficulty is the big size of these engines, which require a considerable number of discretization mesh cells and consequently exigent computational resources. In the recent years, advancements in computer hardware have facilitated the simulation of large geometries, and several publications about CFD studies of large and medium marine engines can be found in the technical literature. One can refer to Kilpinen [14], who studied numerically a medium-speed, four-stroke marine diesel engine, the Wärtsilä 6R20. He simulated different loads and found an increase in NO_x emissions with load. Larbi and Bessrour [15] analyzed numerically the emissions of the Wärtsilä NSD type 6R32 LNE marine engine. After that, they employed the model to study the NO_x reduction by EGR, ammonia injection and water injection, [16-18] respectively. Kontoulis *et al.* [19] analyzed advanced injection strategies to reduce NO_x emissions in the Sulzer

RTA58T marine engine. Leng *et al.* [20] studied numerically the effect of the modulate injection in the SEMT Pielstick 6PC2.6 medium speed marine engine. They concluded that NO_x emissions are lower when a boot-type injection is employed. Andreadis *et al.* [21] simulated a pilot injection in the Sulzer RT-flex58T-B. Kyriakides [22] studied two different nozzle sizes in the Sulzer RT-flex58T-B marine engine.

Due to the current regional, national and international legislation about emissions from marine engines, the reduction of pollutants remains a priority for engine designers. The most relevant legislation is the IMO Marpol Annex VI, which limits the content of sulfur in fuels and indicates maximum allowable NO_x emissions for marine ships built alter 2000, 2011 and 2016 [23]. In this regard, CFD is very useful to study the capability of NO_x reduction measurements. An accurate numerical prediction of NO_x allows engine designers to minimize the need for expensive testing. For this reason, it is very important to simulate marine engines in order to validate and perform the method. For the purpose, the aim of the present paper is to illustrate how a CFD model can simulate the combustion process of the MAN B&W 7S50MC marine engine. As NO_x reduction measurements, EGR (exhaust gas recirculation) and water addition were analyzed. The numerical results were validated with experimental measurements of the in-cylinder pressure on a MAN B&W 7S50MC installed on a container ship. These measurements were carried out by the authors of the present paper. The value of NO_x emission was not experimentally measured, but it was obtained from MAN B&W [24]. A satisfactory agreement between numerical and experimental results was resulted.

2. CASE STUDIED

The MAN B&W 7S50MC studied in the present work is a two-stroke, low speed, marine diesel engine with 7 cylinders, 50 cm bore, 191 cm stroke, 375028 cm^3 cylinder displacement volume and 127 rpm engine speed. The scavenging process of this engine was modelled in a previous paper [25].

This work was developed at 75% load, for which the indicated power is 7789 kW and the consumption 168 g/kWh (24.5 g of fuel injected per cycle and cylinder). The fuel employed was heavy fuel oil (RMG 380 according to ISO 8217).

This is a direct injection engine (fuel is injected directly into the combustion chamber). Figure 1 shows a lateral and top view of the cylinder head. As can be seen, two fuel injectors are located near the outer edge of the combustion chamber. The fuel is sprayed into the cylinder towards the end of the compression stroke. As the air inside the cylinder remains at high pressure and temperature, the droplets of fuel vaporize and mix with this air. After that, ignition takes place. Atomization, vaporization, fuel-air mixing and combustion continue until all the necessary fuel has passed through each process.

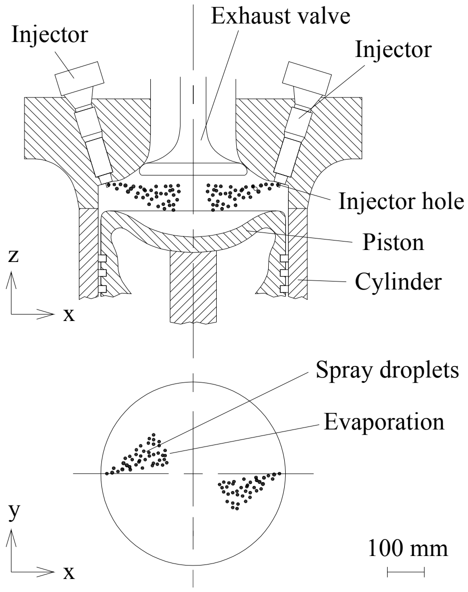

Figure 1. Schematic representation of the spray injection.

3. NUMERICAL PROCEDURE

The numerical computations were performed by means of the open software OpenFOAM, which is based on the finite volume procedure. The CFD simulation was carried out from 20º before TDC (top dead center) to the exhaust valve opening, 120º after TDC. As all cylinders are identical, only one of them was simulated. The inlet ports and exhaust valve are closed during the entire simulation.

3.1 GOVERNING EQUATIONS

In this engine, the cylinder is full of air (or a mixture of air and exhaust gases when EGR is considered) before the injection of fuel, and combustion takes place as the fuel is being injected. This is known as non-premixed combustion (in contrast to premixed combustion, in which fuel and oxidant are mixed before combustion takes place). In non-premixed combustion, the rate of combustion is controlled by the rate at which fuel and air mix. Under such hypothesis, the transport equation which characterizes the propagation of the flame front is given by:

$$\frac{\partial}{\partial t}(\rho f)+\frac{\partial}{\partial x_i}(\rho u_i f)=\frac{\partial}{\partial x_i}\left(\frac{\mu_t}{\sigma_\xi}\frac{\partial f}{\partial x_i}\right) \tag{1}$$

In this equation, f (the mixture fraction) is the local mass fraction of burnt and unburnt fuel stream elements (C, H, etc) in all the species (CO_2, H_2O, O_2, etc). For the following chemical reaction, in which C represents the fuel, O the oxidant and P the products:

$$\phi C + rO \rightarrow (\phi + r)P \tag{2}$$

the mixture fraction is given by:

$$f = \frac{\phi}{\phi + r} \tag{3}$$

The equations of conservation of mass, momentum and energy are needed too, Eqs. (4) to (6) respectively:

$$\frac{\partial \rho}{\partial t} + \frac{\partial}{\partial x_i}(\rho u_i) = 0 \tag{4}$$

$$\frac{\partial}{\partial t}(\rho u_i) + \frac{\partial}{\partial x_j}(\rho u_i u_j) = -\frac{\partial p}{\partial x_i} + \frac{\partial \tau_{ij}}{\partial x_j} + \frac{\partial}{\partial x_j}(-\rho \overline{u_i' u_j'}) \tag{5}$$

$$\frac{\partial}{\partial t}(\rho H) + \frac{\partial}{\partial x_i}(\rho u_i H) = \frac{\partial}{\partial x_i}\left[\left(\frac{\mu}{\sigma} + \frac{\mu_t}{\sigma_h}\right)\frac{\partial H}{\partial x_i}\right] + S_{rad} \tag{6}$$

In the equations above, the term $(-\rho \overline{u_i' u_j'})$ represents the Reynolds stresses, modelled by the *k-ε* turbulence model. S_{rad} is a source term to include the radiation heat transfer, computed by the *P1* model.

Concerning the chemical species, these were characterized using the concept of chemical equilibrium (the chemical kinetics is so fast that equilibrium is reached quickly). The following 20 chemical species were considered: $C_{12}H_{23}$ (fuel), O_2, N_2, CO_2, H_2O, CO, C, CH_4, O, H, H_2, H_2O_2, N, OH, HO_2, HNO, HONO, C_2H_6, HCO and CHO.

The reactions of formation of NO_x are not fast enough to consider chemical equilibrium. For this reason, its treatment was decoupled from the combustion model. Among the NO_x components, NO is the main pollutant (nearly 100% of NO_x is NO). Almost all NO is generated by the reactions proposed by Zeldovich [26], reactions (7) and (8), and Lavoie [27], reaction (9).

$$\mathrm{O+N_2} \underset{k_{-1}}{\overset{k_1}{\rightleftarrows}} \mathrm{NO+N} \tag{7}$$

$$\mathrm{N+O_2} \underset{k_{-2}}{\overset{k_2}{\rightleftarrows}} \mathrm{NO+O} \tag{8}$$

$$\mathrm{N+OH} \underset{k_{-3}}{\overset{k_3}{\rightleftarrows}} \mathrm{NO+H} \tag{9}$$

The rate of formation of NO is given as follows:

$$\frac{d[\mathrm{NO}]}{dt} = k_1[\mathrm{O}][\mathrm{N_2}] + k_2[\mathrm{N}][\mathrm{O_2}] + k_3[\mathrm{N}][\mathrm{OH}] - k_{-1}[\mathrm{NO}][\mathrm{N}] - k_{-2}[\mathrm{NO}][\mathrm{O}] - k_{-3}[\mathrm{NO}][\mathrm{H}] \tag{10}$$

where [NO], [O], [N_2], [N], [O_2], [OH] and [H] are the concentrations, mol/m^3; k_1, k_2, k_3 are the rate constants and k_{-1}, k_{-2}, k_{-3} are the corresponding reverse rates. The forward and backward reaction rate constants for these three key reactions are given by:

$$\begin{aligned} k_1 &= 1,8x10^{11} e^{(-38370/T)} \\ k_2 &= 1,8x10^{7} Te^{(-4680/T)} \\ k_3 &= 7,1x10^{10} e^{(-450/T)} \\ k_{-1} &= 3,8x10^{10} e^{(-425/T)} \\ k_{-2} &= 3,8x10^{6} Te^{(-20820/T)} \\ k_{-3} &= 1,7x10^{11} e^{(-24560/T)} \end{aligned} \tag{11}$$

3.2 BOUNDARY CONDITIONS

The piston is refrigerated by oil, while the cylinder and cylinder head are refrigerated by water. This heat transfer was modeled as a combined convection-radiation type, given by the following equation:

$$q = h(T_{gas} - T_{refrigerant}) \tag{12}$$

where q is the heat transferred, T_{gas} is the in-cylinder temperature, $T_{refrigerant}$ is temperature of the refrigerant, which was experimentally measured by the authors of the present paper (350.1 K the cooling water and 326.7 K the cooling oil) and h is the heat transfer coefficient, given by the following expression, Taylor [28]:

$$h = 10.4kb^{-1/4}(u_{piston}/\nu)^{3/4} \tag{13}$$

where b is the cylinder bore, k the thermal conductivity of the gas, u_{piston} the mean piston speed and ν the kinematic viscosity of the gas. Substituting values into the above equation yields $h = 3557$ W/m^{2}K.

3.3 COMPUTATIONAL GRID

The CAD 3D design was performed using SolidEdge ST software and the mesh using Gambit 2.4. In order to model the movement of the piston, a moving grid was employed. Figure 2 shows the grid at the start of the simulation, 20º before TDC, and at TDC. As can be seen, only the combustion chamber was simulated. The exhaust valve and intake ports were not meshed because they remain closed during the entire simulation.

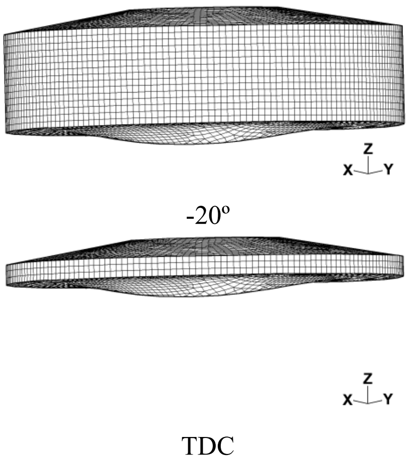

Figure 2. Computational grid at 20º and TDC crankshaft angles.

A hexahedral mesh was employed. The number of elements varies from about 260000 at the start of simulation to 65000 at TDC. In order to ensure grid independence, five meshes were compared. The number of elements of these meshes at the start of simulation was 100000, 150000, 200000, 240000 and 260000. The results provided by the 240000 and 260000 elements were practically identical. For this reason, the mesh with 260000 elements at the start of simulation was adopted for the present work.

3.4 NUMERICAL ASPECTS

The CFD software employed in this work, OpenFOAM, is basically a C++ library for numerical simulation of fluid mechanic problems. The governing equations of the present work were programmed from an extension of the solver dieselEngineFoam, thereby developing a new CFD solver. DieselEngineFoam implements the injection of spray fuel and droplet evaporation by means of momentum sources in the mass, momentum and energy conservation equations.

As injection properties, a 10 µm diameter and 20º spray angle were employed because these are common values on a wide range of engines [29-31]. The injected mass was obtained from the consumption, 168 g/kWh (24.5 g of fuel injected per cycle and cylinder). The fuel temperature, 408K, was obtained from experimental measurements carried out by the authors of the present paper.

Chemical reactions are not implemented in the solver dieselEngineFoam and must be included by the user. For the purpose, Eq. (1) was added to the code. Concerning NO_x formation, another transport equation was added to the code in order to compute the mass fraction of NO, Eq. (14), Versteeg and Malalasekera [32]:

$$\frac{\partial}{\partial t}(\rho f_{NO}) + \frac{\partial}{\partial x_i}(\rho u_i f_{NO}) = \frac{\partial}{\partial x_i}\left(\frac{\mu_t}{\sigma_\xi}\frac{\partial f_{NO}}{\partial x_i}\right) + S_{NO} \quad (14)$$

where f_{NO} is the mass fraction of NO and S_{NO} is a source to represent the mean rate of production of NO, which can be evaluated by the following equation:

$$S_{NO} = M_{NO}\frac{d[NO]}{dt} \quad (15)$$

where M_{NO} is the molecular weight of NO and $d[NO]/dt$ is the molar rate of creation/destruction of NO, computed from Eq. (10).

The PISO algorithm was chosen for pressure-velocity coupling. A second order scheme was chosen to discretize the continuity, momentum, energy, and mass fraction equations. The time derivatives were discretized through a first order fully implicit scheme with a constant time step of 0.0005 s. As in the case of the number of mesh elements, several simulations were performed with different values of the time step in order to ensure independence of this value.

4. RESULTS

The spray and mass fraction of fuel are shown in Figure. 3. For the conditions studied, injection of fuel takes place from -2º to 13º crankshaft angle. 0º, 5º and 15º crankshaft angles were represented in Figure. 3. As can be seen, the fuel spray enters the cylinder as liquid drops. The structure of each fuel spray is that of a narrow liquid-containing core surrounded by a much larger gaseous-jet region containing fuel vapour. After the injection of fuel, the flame extinguishes progressively.

The temperature field is shown in Figure. 4. As can be seen, the temperature increases as combustion takes place. Near the TDC, the temperature also rises due to the high pressure.

Unfortunately, the numerical results of temperature were not validated with experimental data because the response time of temperature sensors is not fast enough to characterize the evolution along the cycle of operation. Besides, the temperature field is highly non-uniform and consequently very difficult to measure. Nevertheless, it was verified that the maximum temperature obtained numerically agree with the values suggested in several books of engines [31, 33, 34].

Figure 5 shows numerical and experimental in-cylinder pressure traces. The in-cylinder pressured was measured experimentally by the authors of the present paper. The injection pressure, obtained from MAN B&W [24], is also shown in this figure. As can be seen, the modelled in-cylinder pressure data shows good agreement with experimental results.

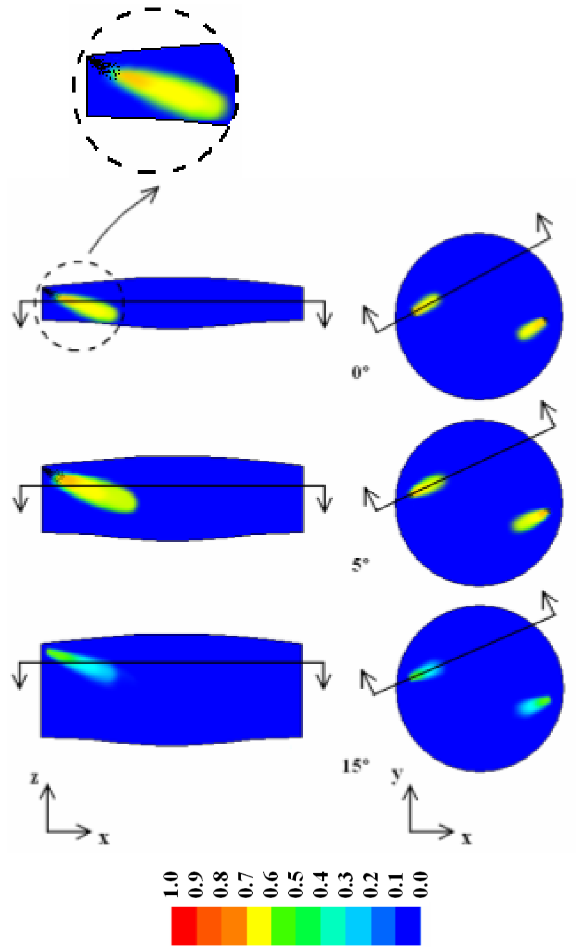

Figure 3. Spray and mass fraction of fuel.

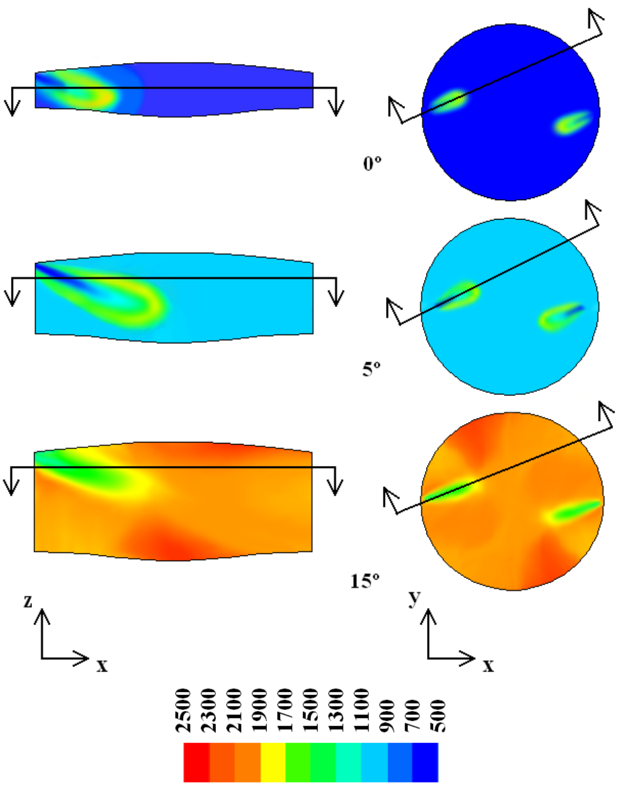

Figure 4. Temperature field (K).

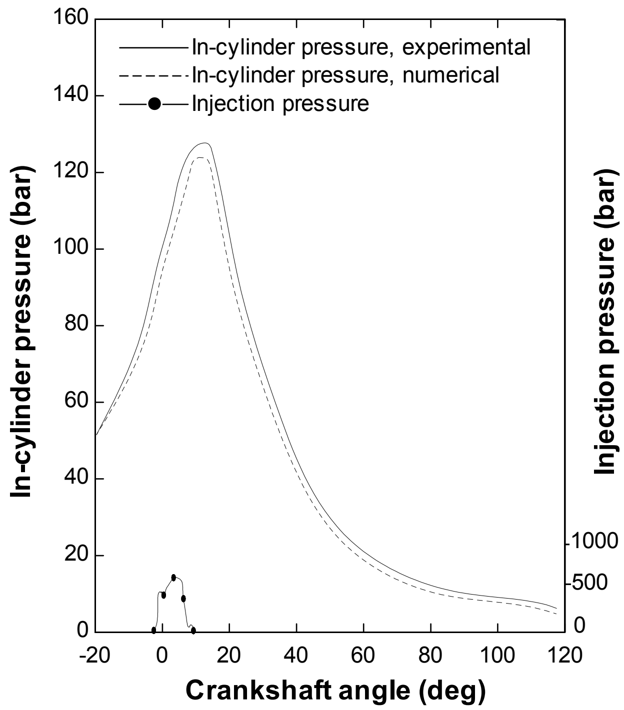

Figure 5. In-cylinder and injection pressure.

The pollutant emissions predicted by the CFD code were 11.1% vol. of CO_2, 118 ppm vol. of CO, 472 ppm vol. of HC and 887 ppm vol. of NO_x. According to MAN B&W [24], at 75% load the engine emits 973 ppm vol. of NO_x, which suppose an error of 8.8% with respect to the numerical result. This error is quite acceptable considering the difficulty of simulating the combustion process. Besides, marine engines have several adjustments (fuel temperature, valve timing, turbocharger pressure, etc) which can have repercussions on the results. Concerning the emissions of CO_2, CO and HC, these agree with the usual values for two-stroke low speed marine engines suggested elsewhere [35-36].

The value of NO_x emissions, 887 ppm, corresponds to 14.9 g/kWh, which sticks the IMO TIER I but not IMO TIER II. Nowadays, MAN B&W and other companies incorporate advanced methods to reduce NO_x and other pollutants. As mentioned previously, NO_x is formed from oxygen and nitrogen due to the high temperatures reached during the combustion process. Equations (10) and (11) indicate that the reactions of NO formation are very dependent on the temperature and concentrations of nitrogen and oxygen. For this reason, NO_x reduction measurements focus on lowering the concentrations of nitrogen and oxygen, peak temperatures and the amount of time in which the combustion gases remain at high temperatures. In the following section, two common NO_x reduction measurements are numerically analyzed, EGR and water addition.

5. EGR AND WATER ADDITION

Introduction of water or exhaust gases into the combustion chamber reduces combustion temperature due to an increase in the specific heat capacity of the cylinder gases (H_2O and gas have higher specific heat capacity than air) and a reduced overall oxygen concentration.

5.1 EGR (EXHAUST GAS RECIRCULATION)

Exhaust gas recirculation is a method of modifying the inlet air. It consists on recirculating a fraction of the exhaust gases to the engine intake system. Logically, only a small proportion of the injected exhaust gas is present in the combustion region.

In order to study the effect of EGR in this work, the initial conditions were modified to a mixture of gas-air instead air alone. The relative changes in NO_x, CO and HC emissions against the gas to air ratio are shown in Fig. 6. In this figure, the EGR rate is the mass ratio between the recirculated exhaust gas and the total gas in the cylinder.

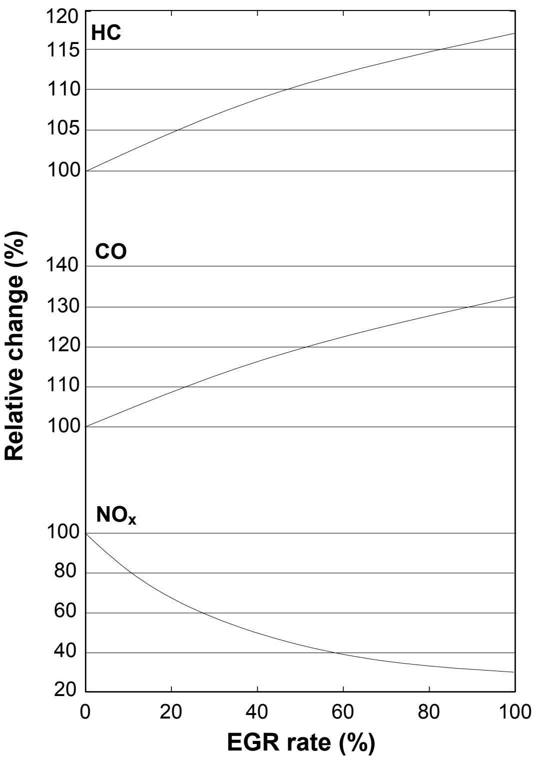

Figure 6. Relative change in pollutants against gas to air ratio.

As can be seen in Figure. 6, EGR reduces NO_x emissions but increases both HC and CO emissions. The increase in HC and CO is caused by the lower temperatures, which promote slow combustion and partial burning.

It is important to mention that practical applications do not reach more than 50% EGR rate [34-35]. Nevertheless, the numerical simulations were carried out up to 100% EGR rate in order to indicate the capability of EGR to reduce NO_x emissions.

5.2 WATER ADDITION

Water addition is another common measure to reduce NO_x. It consists on introducing water in the combustion chamber in order to lower the peak temperature. Water can be introduced as humidity in the charge air, directly or through a water-fuel emulsion.

In this work, the effect of water was studied by carrying out simulations using a water-fuel emulsion instead a pure fuel injection. The results of relative change in NO_x, CO and HC against the water to fuel ratio are shown in Fig. 7. In this figure, the water to fuel ratio is the ratio of water mass to fuel mass.

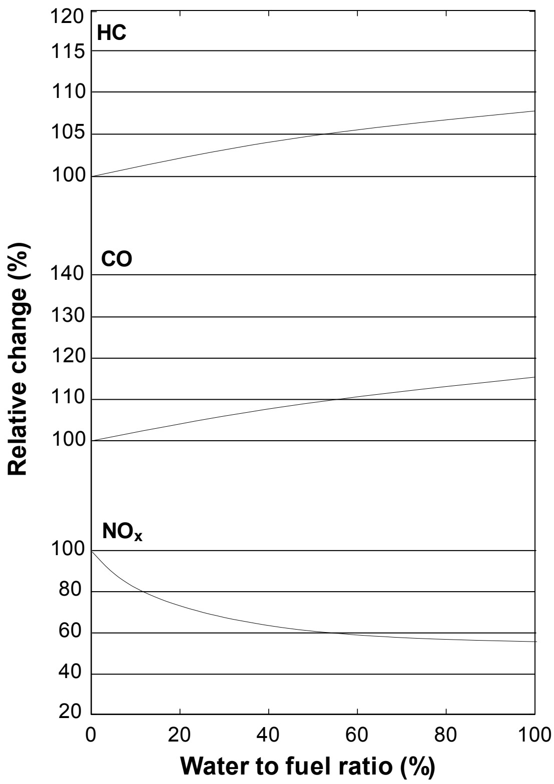

Figure 7. Relative change in pollutants against water to fuel ratio.

As can be seen in Figure. 7, as the quantity of added water is increased, NO_x is reduced but CO and HC are increased. The reasons are the same as in the case of EGR.

As in the case of EGR, a water to fuel ratio of 100% is unrealistic in practical applications. Typical water to fuel ratios are 40-70% [35]. A 100% was analyzed simply to indicate the capability of water addition to reduce NO_x emissions.

Unfortunately, the results shown in Figures. 7 and 8 were not validated experimentally. Nevertheless, it was verified that the tendency of the curves coincide with other experimental data carried out elsewhere [34].

6. CONCLUSIONS

The present paper proposes a CFD model to simulate the combustion process and characterize the exhaust gasses composition of a marine engine. The strongest motivation is given by the current legislation, for which the most important gas component that must be reduced in marine diesel engines is NO_x. As measures to reduce NO_x, EGR and water addition were analyzed.

The engine studied was the MAN B&W 7S50MC. A good agreement between the modelling and experimental data ensures the accuracy of the numerical predictions developed in this investigation. Experimental measurements of the in-cylinder pressure were carried out in a MAN B&W 7S50MC installed on a container ship.

In future works, the purpose is to employ this model to study several parameters such as combustion chamber geometry, compression ratio, etc, as well as more NO_x reduction measurements.

7. ACKNOWLEDGEMENTS

The authors would like to express their gratitude to “Talleres Pineiro, S.L.”, marine engines maintenance and repair shop.

8. REFERENCES

1. SKJOLSVIK, K.O.; ANDERSEN, A.B.; CORBETT, J.J.; SKJELVIK, J.M., Study on greenhouse gas emissions from ships. *Final Report to the International Maritime Organization, MT Rep. Mtoo A23-038, MARINTEK, Trondheim, Norway*, 2000.
2. PRIESCHING, P.; WANKER, R.; CARTELLIERI, P.; TATSCHI, R. Detailed and reduced chemistry CFD modeling of premixed charge compression ignition engine combustion. *International Multidimensional Engine Modeling user’s Group Meeting*, 2003.
3. KONGRE, U.V.; SUNNAPWAR, V.K. CFD modeling and experimental validation of combustion in direct ignition engine fueled with diesel. *International Journal of Applied Engineering Research, volume 1(3)*, 2010.
4. RINALDINI, C.A.; MATTARELLI, E.; GOLOVITCHEV, V. CFD Analyses on 2-stroke high speed diesel engines. *SAE International Journal of Engines. volume 4(2), pp. 2240-2256*, 2011.
5. ISMAIL, H.M.; NG, H.K.; GAN, S. Evaluation of non-premixed combustion and fuel spray models for in-cylinder diesel engine simulation. *Applied Energy, volume 90(1),* 2011.
6. ZHAO-JIE, S.; LIU, Z.C.; YONG, H.; WANG, Z.; LIU, J. Simulation on two-stage injection combustion of diesel engine under light load. *International Conference on Computer Distributed Control and Intelligent Environmental Monitoring*, 2011.
7. REITZ, R.D.; RUTLAND, C.J. Development and testing of diesel engine CFD models. *Progress in Energy and Combustion Science, volume, 21, pp. 173-196*, 1995.
8. SHENGI, L.; HEKUN, J.; BIFENG, Y.; ZHENWEI, X.; TAO, G. Numerical simulation on the effect of pilot injection on combustion and NO_x emission characteristics of light-vehicle diesel engine. *International Conference on Computer Distributed Control and Intelligent Environmental Monitoring*, 2011.
9. PENG, Z.; LIU, B.; WANG, W.; LU, L. CFD investigation into diesel PCCI combustion with optimized fuel injection. *Energies, volume 4, pp. 517-531*, 2011.
10. ABDULLAH, S.; KURNIAWAN, W.H.; KHAMAS, M.; ALI, Y. Emission analysis of a compressed natural gas direct injection engine with a homogeneous mixture. *International Journal of Automotive Technology, volume 12, pp. 29-38*, 2011.
11. LUO, M.; XIANG, L.; LI, X. Numerical simulation of the effects of combustion chamber geometry on nonroad diesel engine performance. *International Conference on Electric Information and Control Engineering*, 2011.
12. BIGOS, P.; PUSKAR, M. Influence of cylinder shape and combustion space on engine output characteristic of two-stroke combustion engine. *Zdvihací zařízení v teorii a praxi* 3, 2008.
13. ULUDOGAN, A.; XIN, J.; REITZ, R.D. Exploring the use of multiple injectors and split injection to reduce DI diesel engine emissions. *SAE Paper 962058*, 1996.
14. KILPINEN, P. Optimization of a simplified sub model for NO emission prediction by CFD in large 4-stroke marine diesel engines. *Fuel Processing Technology, volume 91(2), pp. 218–228*, 2010.
15. LARBI, N.; BESSROUR, J. Experimental measure and simulation of pollutant emissions from marine diesel engine. *Physical and Chemical News. volume 45(1), pp 80-90,* 2009.
16. LARBI, N.; BESSROUR, J. Measurement and simulation of pollutant emissions from marine diesel combustion engine and their reduction by ammonia injection. *Advances in Mechanical Engineering. 459813*, 2009.
17. LARBI, N.; BESSROUR, J. Measurement and simulation of pollutant emissions from marine diesel combustion engine and their reduction by exhaust gas recirculation. *Journal of Mechanical Science and Technology, volume 22, pp. 2263-2273*, 2008.
18. LARBI, N.; BESSROUR, J. Measurement and simulation of pollutant emissions from marine

diesel combustion engine and their reduction by water injection. *Advances in Engineering Software. volume 41(6), pp. 898-906*, 2010.

19. KONTOULIS, P.; CHRYSSAKIS, C.; KAIKTSIS, L. Analysis of combustion and emissions in a large two-stroke marine diesel engine, using CFD and T-φ mapping, 1*8th International Multidimensional Engine Modeling User's Group Meeting at the Society of Automotive Engineers Congress, Detroit, MI*, 2008.
20. LENG, X. Y.; LONG, W. Q.; FENG, L. Y.; DONG, Q.; LI, H. Y.; WANG, X. J.; YU, X. J.; WANG, A. G. Numerical simulation research into effects of injection rates on performance and emissions of diesel engine. *Journal of Dalian University of Technology, volume 51(2), pp. 180–187*, 2011.
21. ANDREADIS, P.; ZOMPANAKIS, A.; CHRYSSAKIS, C.; KAIKTSIS, L. Effects of the fuel injection parameters on the performance and emissions formation in a large-bore marine diesel engine, *International Journal of Engine Research, volume12(1), pp. 14–29*, 2011.
22. KYRIAKIDES, N.; CHRYSSAKIS, C.; KAIKTSIS, L. Development of a computational model for heavy fuel oil for marine diesel engine applications. *19th International Multidimensional Engine Modeling User's Group Meeting at the SAE Congress, Detroit, MI*, 2009.
23. LAMAS, M.I.; RODRIGUEZ, C. Emissions from marine engines and NO_x reduction methods, *Journal of Maritime Research, volume 9(1), pp. 77-82*, 2012.
24. http://www.mandieselturbo.com
25. LAMAS, M.I.; RODRÍGUEZ VIDAL, C.G., Computational fluid dynamics analysis of the scavenging process in the MAN B&W 7S50MC two-stroke marine diesel engine, *Journal of Ship Research*, *volume 56(3), pp 154–161*, 2012.
26. ZELDOVITCH, Y.B.; SADOVNIKOV, D.A.; KAMENETSKII, F. Oxidation of nitrogen in combustion. *Institute of Chemical Physics, Moscow-Leningrad,* 1947.
27. LAVOIE, G.A.; HEYWOOD, J.B.; KECK, J.C., Experimental and theoretical investigation of nitric oxide formation in internal combustion engines. *Combustion Science Technology, volume 1, pp 313-326*, 1970.
28. TAYLOR, C.F. The internal combustion engine in theory and practice. *2nd Edition. MIT Press*, 1985.
29. HEIWOOD J. B. Internal combustion engine fundamentals. *McGraw-Hill, 1988.*
30. CHALLEN B.; BARANESCU R. Diesel engine reference book. *2nd Edition. Society of Automotive Engineers*, 1999.
31. GARCIA OLIVER J.M. El proceso de combustión turbulenta de chorros diesel de inyección directa. *1st Edition. Editorial Reverté, Spain,* 2006.
32. VERSTEEG, H.K.; MALALASEKERA, W. An introduction to computational fluid dynamics the finite volume method, *2nd Edition, Pearson Prentice Hall*, 2007.
33. [33] BLAIR G.P. Design and Simulation of Two-Stroke Engines. *SAE International*, 1996.
34. [34] PAYRI F.; DESANTES, J.M., Motores de combustión interna alternativos. *1st Edition. Editorial Reverté, Spain,* 2011.
35. WOODYARD, D. Pounder's marine engines and gas turbines. *8th edition. Oxford, Elsevier*. 2004.
36. KUIKEN, K. Diesel engines for ship propulsion and power plants from 0 to 100000 kW. *Target Global Energy Training. 1st edition. The Netherlands*. 2008.

